43rd IEEE Conference on Decision and Control
December 14-17, 2004
Atlantis, Paradise Island, Bahamas

Digitizing Method with Application to the Design of Fractional-Time Prediction Models

Grigore I. Braileanu, *Senior Member, IEEE*

Abstract – **An interpolation based digitizing method has been previously developed especially for the design of narrowband frequency selective filters. This method performs a trigonometric polynomial interpolation along an extended time window that ends at the current sampling time. The present paper reconsiders the basic extended window design (EWD) idea in the light of digital control systems requirements and proposes a generalized EWD (G-EWD) method. The main results of this paper are: (i) the closed-form G-EWD expressions derived for an interpolation space spanned by any set of linearly independent functions of time, (ii) a computationally efficient linear algebra generation of the G-EWD digital equivalents, and (iii) the derivation of optional prediction models whose output values are computed at fractional time instants beyond the current sampling time. Finally, the paper compares the proposed G-EWD method to an optimal frequency-domain digitizing method.**[1]

I. INTRODUCTION

A near-optimal method for the design of discrete-time equivalents of analog systems, based on trigonometric polynomial interpolation along an extended time window that ends at the current sampling time, was recently introduced [1]. This method, referred to in the following as the T-EWD, was developed especially for the design of narrowband frequency selective filters and was proven in [2] to be equivalent to the optimal iterative weighted least squares (WLS) design [3] of conventional digital filters.

At the same time, the T-EWD filters are characterized by additional features. Specifically, in contrast to the filter design performed directly in the digital domain, the nature of the EWD digitizing equations, which approximate the continuous-time output of analog filters, leads to a dramatic reduction of the digitizing error by adding a fractional delay or by increasing the filter order while the additional poles are placed at z=0. Yet, a significantly different problem occurs in digital control systems. First, the performance specifications are mainly given in the time-domain, and only to a lesser extent in the frequency domain. Second, unlike digital signal processing applications, which usually allow for off-line computations where delays usually do not matter, the delays in control systems are prohibitive. At the same time, in digital control systems a fractional-time prediction is highly desirable in order to compensate for both the latency in computing the control law and the delay due to the hold element of the D/A converter. In the following, a new digitizing method, referred to as the generalized extended window design (G-EWD) is proposed in a form that addresses the control system requirements, including an optional fractional-time prediction.

Basically, the traditional two-point linear interpolation method for digitizing analog systems [4],[5] – that produces the so-called triangle-hold equivalents – was modified in [1] in order to use (m+1)-point interpolators with $m \geq 2$. This design consists in the following: (i) a composition of the interpolation and filtering operators into just one operator by incorporating the interpolation step into the s- to z-domain mapping step (as opposed to a sequential approach that would cascade the interpolator and the analog system), (ii) the use of trigonometric polynomials for interpolation, and (iii) digital implementations with an optional delay d and additional poles at z=0. The order of the resulting digital transfer function $H_D(z)$ is $m \geq n_A+d$, where n_A is the order of the analog system defined by its transfer function $H(s)$. It was shown that the features (i)-(iii) are relevant only for $m \geq 2$, and they increase the digitizing accuracy as m increases within reasonable limits.

The above idea of an extended interpolation interval is used by the G-EWD method proposed below, but modified in two ways. First, the interpolation interval is additionally extended to the right with a fractional-time prediction interval. Second, the interpolation space spanned by a restricted set of sinusoidal functions is replaced with the space generated by a finite set of selected linearly independent functions of time $\{\phi_0(t),...,\phi_m(t)\}$. In the case of digital control system design, a particular attention is given to the modes of the analog model that will form the basis of the interpolation space. Accordingly, given a transfer function $H(s)$, the proposed design produces a particular digital equivalent defined through two sets of equations: a conventional I/O recursive equation associated with a transfer function $H_D(z)$ and a small size fractional-time prediction vector that can be stored with reduced-word arithmetic. The process that leads to these equations is now briefly presented with reference to Fig. 1. Throughout the paper, the time is assumed to be normalized to the sampling period T_s of the input signal, and so the *folding frequency* will be $\omega_f = \pi$ unless otherwise specified.

The author is with the Electrical and Computer Engineering Department, Gonzaga University, Spokane, WA 99258, USA (phone: 509-323-3536, fax: 509-323-5871, e-mail: braileanu@gonzaga.edu)

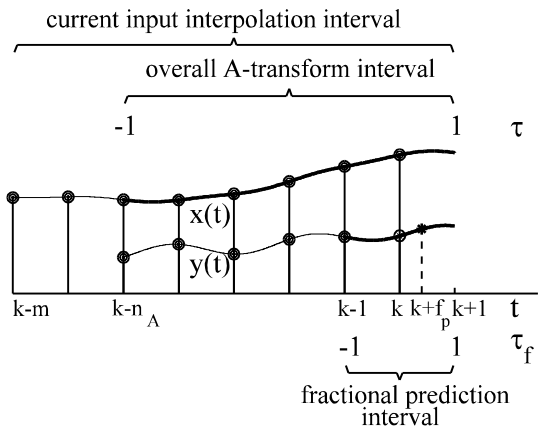

Fig. 1. Interpolation intervals for m=7, n_A=5, and f_p=0.3. Definitions of some normalized variables according to Section III below: t = the time normalized to the sampling period; τ = the A-transform time variable of the *conventional filter* design interval $k\text{-}n_A \le t \le k\text{+}1$; τ_f = the A-transform variable of the fractional prediction interval $k\text{-}1 \le t \le k\text{+}1$.

The recursive generation of the current output $y(k)$ is based on the response $y(t)$, $k\text{-}n_A \le t \le k\text{+}1$, of the analog system $H(s)$ to the interpolated signal $x(t)$ built from the last $(m\text{+}1)$ input samples up to the current time $t=k$. Moreover, $y(t)$ is determined along the time segment, $k\text{-}n_A \le t \le k\text{+}1$, while the initial conditions are the output samples $y(k\text{-}n_A), \ldots, y(k\text{-}1)$ that were computed during the last n_A steps. Thus, this design, referred to as the *extended window design* provides a natural match for the initial conditions of the analog and digital systems and incorporates the interpolation step into the s- to z-domain mapping step. The *current* sets of input and output samples used as *auxiliary conditions* during the computation of the analog filter response are grouped into the vectors $\mathbf{x}_{aux}$ and $\mathbf{y}_{aux}$:

$$\begin{cases} \mathbf{x}_{aux} \triangleq \left[x_k, x_{k-1}, \ldots, x_{k-m} \right]^T, \\ \mathbf{y}_{aux} \triangleq \left[y_{k-1}, y_{k-2}, \ldots, y_{k-n_A} \right]^T . \end{cases} \tag{1}$$

Yet, the salient feature of the G-EWD is its flexibility in generating *accurately predicted output values at fractional time instants* within the interval $k \le t < k\text{+}1$. Specifically, the $(m\text{+}1)$ input samples obtained up to the current time $t=k$, together with the basis functions $\{\phi_0(t), \phi_1(t), \ldots, \phi_m(t)\}$, generate the interpolated signal $x(t)$, $k\text{-}m \le t \le k\text{+}1$. Next, an approximation $y(t)$ of the response of the analog system $H(s)$ to the interpolated signal $x(t)$ is computed on $k\text{-}n_A \le t \le k\text{+}1$ at predetermined fractional time instants as, for example, $t=k+f_P$. Depending on the control system application, the initial conditions used to obtain $y(t)$ may be either $y(k\text{-}n_A), \ldots, y(k\text{-}1)$ if only the latency effect is to be compensated, or $y(k\text{-}n_A\text{+}1), \ldots, y(k\text{-}1), y(k)$ if the prediction is needed after the last output sample $y(k)$ has been collected. The accuracy of the predicted values stems from the fact that the interpolations at equally spaced time instants are accurate around the middle of the interpolation interval [6], while the interpolation error increases toward the end segments. Thus, the *extended time window* used in the computation of $x(t)$, together with the fact that the response $y(t)$ of $H(s)$ is computed after dropping the $(m\text{-}n_A)$ left hand segments, makes $y(t)$ benefit from the increased accuracy of the central segment of $x(t)$ which contains most of the energy of $x(t)$. Here, it should also be noted that, in general, the most current input values (as, for example, on $k \le t \le k\text{+}1$) have little effect on the current output values.

The paper is organized as follows. Section II derives the closed form expression of the transfer functions $H_D(z)$ produced with the generalized extended window design. Section III presents a set of equations derived through linear algebra and numerical methods which demonstrates the efficiency of the EWD approach in implementing a fractional-time prediction. While, algebraically, the T-EWD looks only like a particular case of the G-EWD, Section IV emphasizes the fundamental difference between the T-EWD and a particular G-EWD design that uses the interpolation space spanned by the modes of the analog system $H(s)$. Finally, the proposed digitizing method is compared to the T-EWD and WLS methods in the concluding Section V.

II. THE G-EWD METHOD

The G-EWD method provides digital equivalents of systems defined by transfer functions of the form

$$H(s) = \frac{Y(s)}{X(s)} = \frac{N(s)}{D(s)} = \frac{N(s)}{s^{n_A} + a_1 s^{n_A-1} + \ldots + a_{n_A}} \tag{2}$$

where $N(s)$ and $D(s)$ are known polynomials of orders m_A and n_A, respectively. In the following, the signals $x(t)$ and $y(t)$ are the input and output of the analog system $H(s)$, while the input and output of the designed digital equivalent $H_D(z)$ are denoted by $x_D(k)$ and $y_D(k)$, respectively. The order of $H_D(z)$ is denoted by n_D.

A. The Time-Domain Invariance Synthesis

The principle of time-domain invariance used to digitize analog systems assumes that identical inputs, $x_D(k)=x(t)|_{t=k}$, yield identical outputs, $y_D(k)=y(t)|_{t=k}$, along the entire time axis. Thus, this time-domain equivalence [5] implies the identity of the z-transforms $Y_D(z) \triangleq H_D(z)X_D(z)$ and $Z\{Y(s)\}$. With the notation of [4, Sect. 4.3.1], the expression $Z\{Y(s)\} \triangleq Z\{[\mathcal{L}^{-1}[Y(s)]]|_{t=k}\}$ is the z-transform of the samples of $y(t)$. Thus, the above identity yields the transfer function

$$H_D(z) = \frac{1}{X_D(z)} Z\{Y(s)\} . \tag{3}$$

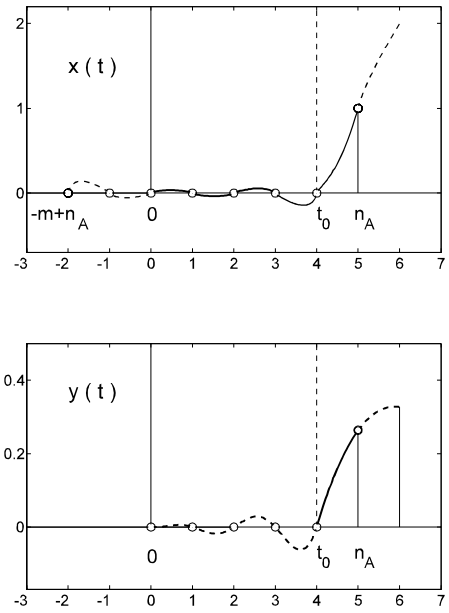

Fig. 2. I/O signals defining the *time-domain invariance synthesis* applied to a time window extended to the left of the current sampling period $[n_A\text{-}1, n_A]$ along $(m\text{-}1)$ sampling steps ($m \geq n_A$), and to the right by one prediction step. The *solid lines* correspond to the I/O conventional equations: the current output $y(n_A)$ is computed from the response of $H(s)$ to the segment $x(t)$, $0 \leq t \leq n_A$, of the $(m+1)$-point interpolation, with the auxiliary conditions $y(0) = y(1) = \ldots = y(n_A\text{-}1) = 0$; t_0 is the time instant where the condition of initial rest applies. The *right end dashed lines* correspond to the prediction.

It was shown in [2] that signals $x(t)$ of the form illustrated in Fig.2 completely characterize a given interpolator. Thus, the crux of the design is the selection of *the characteristic signal* $x(t)$, together with the method for calculating the corresponding response $y(t)$ of the analog system $H(s)$. Particular characteristic signals and time response computations may yield the traditional impulse- and step-invariance methods, the linear interpolation method or, finally, the G-EWD — as shown below. At the same time, the design must satisfy the *condition of initial rest*, which specifies that if the input $x(t)$ is zero for all the time instants prior to some initial time t_0, then the output $y(t)$ must also be zero for $t<t_0$. Fig. 2 illustrates the general shape of the admissible EWD characteristic signals $x(t)$, as well as the corresponding form of the response $y(t)$ of the analog system. The interpolation adds the requirement of continuous input, and so the above condition must also hold for $t=t_0$. Finally, the interpolation implies that $x(t)$ is an analytical function. Therefore, in the context of time-invariant synthesis, the class of *admissible characteristic signals*, $x(t)$, corresponding to an $(m+1)$-point interpolation will be the set of functions whose zeros are m adjacent integers up to and including $t=t_0$. Fig. 2 shows that the time origin is chosen such that there are n_A interpolation segments between $t=0$ and the time instant where the current digital output is computed.

B. Derivation of G-EWD transfer functions

For convenience, the G-EWD interpolation of the input signal will be restricted to a set of linearly independent functions of the form of modes of analog LTI systems. Typically, $x(t)$ is given by

$$x(t) = \sum_{n=1}^{M_1} A_n e^{-p_n t} + \sum_{n=1}^{M_2} e^{-q_n t}(B_n \cos \omega_n t + C_n \sin \omega_n t), \quad (4)$$

or, equivalently, by

$$x(t) = \sum_{n=1}^{m+1} \alpha_n e^{r_n t}, \quad m = M_1 + 2M_2 . \quad (4')$$

Usually, M_1 and M_2 are selected such that $m \geq n_A$ and the coefficients A_n, B_n and C_n are obtained as the *exact solution* of the $(m+1)$ algebraic equations represented in vector form

$$\sum_{n=1}^{M_1} A_n e^{-p_n \mathbf{t}_k} + \sum_{n=1}^{M_2} e^{-q_n \mathbf{t}_k}(B_n \cos \omega_n \mathbf{t}_k + C_n \sin \omega_n \mathbf{t}_k) = \begin{bmatrix} 0 \\ \vdots \\ 0 \\ 1 \end{bmatrix} \quad (5)$$

where $\mathbf{t}_k$ is the vector of sampling times $\mathbf{t}_k = [-m+n_A, \ldots, n_A]^T$, and the right hand side is the vector of the sampled characteristic signal in Fig. 2. Two of the main interpolation space bases are (i) the T-EWD basis composed of sets of sinusoids whose frequencies are chosen within the domain that contains most of the spectral energy of $H(j\omega)$, and (ii) the set containing the *modes* (of oscillation) of the analog system expressed as $q_n(t) = e^{\lambda_n t}$, where λ_n, $n=1,2,\ldots,n_A$ are the poles of $H(s)$. Thus, the first n_A parameters r_n in (4') become $r_n = \lambda_n$, whereas the remaining ones will correspond to sinusoids from the T-EWD basis. Here, for simplicity, λ_n are assumed distinct. Accordingly, the one-sided Laplace and z-transforms of $x(t)$ and its sampled form $x_D(k)$, are given, respectively, by the rational functions

$$X(s) = \frac{R(s)}{Q(s)}, \qquad X_D(z) = \frac{z^{m+1-n_A}}{Q_D(z)}, \quad (6)$$

where both denominators are polynomials with the same degree $(m+1)$. The derivation of $R(s)$ from (4) and (5) is straightforward. Next the simple numerator of $X_D(z)$ is an immediate result of the fact that the characteristic signal is zero at the sampling times $-\infty < t \leq n_A\text{-}1$, while the first nonzero value $x(n_A)=1$ yields $\lim_{z\to\infty} z^{nA} \mathrm{X_D}(z) = 1$. At the same time, the polynomials $Q(s)$ and $Q_D(z)$ are readily defined by their roots. Indeed, the roots of $Q(s)$ are precisely the parameters r_n in (4'), whereas the roots of $Q_D(z)$ are $z_n = e^{r_n}$.

Finally, the EWD transfer function computation assumes the auxiliary conditions $y(t)=0$, for $t = 0, 1, \ldots, n_A\text{-}1$, as illustrated in Fig. 2. This means that the expression of $Y(s)$ in (3) exhibits both a zero-state and a zero-input component: $Y(s)=Y_{zs}(s)+Y_{zi}(s) = X(s)H(s)+Y_{zi}(s)$. In fact, $y_{zi}(t)$ is a linear combination of the modes of $H(s)$, and its coefficients, say, c_k are calculated as to satisfy the auxiliary conditions of the differential equation. The design formula (3) is implemented below by using (2) and (6), and applying the Z operator to both terms of $Y(s)$.

A first result is

$$Z\{X(s)H(s)\} = Z\left\{\frac{R(s)\,H(s)}{Q(s)}\right\} \triangleq Z\left\{\frac{b_0 s^{n_A+m-1} + \ldots + b_{n_A+m-1}}{Q(s)\,(s^{n_A} + a_1 s^{n_A-1} + \ldots + a_{n_A})}\right\} \triangleq \frac{z\,(\beta_0 z^{n_A+m} + \ldots + \beta_{n_A+m})}{Q_D(z)\,(z^{n_A} + g_1 z^{n_A-1} + \ldots + g_{n_A})}, \tag{7}$$

where the polynomial $z^{nA} + g_1 z^{nA-1} + ... + g_{nA}$ is defined by its roots $z_n = e^{\lambda_n}$. Then, the transfer function $H_D(z)$ becomes

$$H_D(z) = \frac{Q_D(z)}{z^{m+1-n_A}}\left[\frac{z(\beta_0 z^{n_A+m} + \ldots + \beta_{n_A+m})}{Q_D(z)\,(z^{n_A} + g_1 z^{n_A-1} + \ldots + g_{n_A})} + \frac{z\,(c_1 z^{n_A-1} + \ldots + c_{n_A})}{z^{n_A} + g_1 z^{n_A-1} + \ldots + g_{n_A}}\right]. \tag{8}$$

The recursive equations below determine the coefficients c_k such that the n_A leading terms of the numerator of $H_D(z)$ in (8) are canceled, thus satisfying the initial conditions:

$$Q_D(z) \triangleq z^{m+1} + d_1 z^m + \ldots + d_{m+1}, \quad c_1 = -\beta_0, \quad \left\{c_k = -\beta_{k-1} - \sum_{n=1}^{k-1} c_{k-n}\, d_n\,, \quad k = 2, \ldots, n_A\right\}. \tag{9}$$

The algebraic analysis of (8) yields Property P1 below.

Property P1: The real-time implementation of the G-EWD transfer function is of order $n_D = m \geq n_A$, with the n_A poles z_n related to the poles λ_n of the analog prototype by the expression $z_n = e^{\lambda_n}$, while the remaining poles, if any, are placed at z=0.

III. THE FRACTIONAL-TIME PREDICTION FORM OF THE G-EWD EQUATIONS

In order to evidence the fractional-time prediction features of the G-EWD method, this section outlines the modifications of the original design of the T- EWD equivalents [1] which used the Chebyshev series representation of signals in terms of vectors of Chebyshev series coefficients. For convenience, this mapping of square integrable functions into the space of square summable vectors defined over the field of real numbers was referred to as the *A*-transformation [7]. Basically, the A-transform **y** of a signal $y(t)$, $t \in [T_1, T_2]$, is the vector $\mathbf{y}=Ay(t)$, whose components are the coefficients of the Chebyshev series expansion of $y(t)$. The inverse *A*-transform is defined by

$$y(t) = [0.5, c_1(\tau), c_2(\tau), \ldots]\,\mathbf{y}, \quad \tau = \frac{2\,t-(T_2+T_1)}{T_2-T_1}, \tag{10}$$

where $c_n(\tau) = \cos(n \arccos \tau)$ are the Chebyshev polynomials of the first kind, and τ is a normalized time variable. It is worth noting that, for any given τ and length N_y of **y**, *only* N_y *multiplications are required*. Indeed, the Clenshaw algorithm which is used to compute (10), does not need the explicit computation of the values $c_n(\tau)$. For example, the *A*-transform of $y(t)$ is may be defined on the interval k-$n_A \leq t \leq k$+1, in order to include the prediction segment as in Fig. 1, or only on k-$n_A \leq t \leq k$, if the design is restricted to the derivation of the I/O digital equivalent $H_D(z)$). Assume now that **y** is the *A*-transform of the output signal $y(t)$ of an analog system, defined in Fig. 1 on the interval k-$n_A \leq t \leq k$+1, corresponding to $-1 \leq \tau \leq 1$. Then, this vector, restricted to the first N_c coefficients may be used to generate the vector $\mathbf{y}_0$ of the interpolated output,

$$\mathbf{y}_o = \mathbf{P}_o\,\mathbf{y}, \quad \mathbf{P}_o: N_o \times N_c, \tag{11}$$

calculated at any given times $t_o = \{t_i\}_{i\,=\,1,2,\ldots,No}$ contained in interval $[k\text{-}n_A, k\text{+}1]$. The i^{th} row of the interpolation matrix P_o is $[0.5, c_1(\tau_i), c_2(\tau_i), \ldots]$ calculated with (10), where $T_1=k\text{-}n_A$, $T_2=k\text{+}1$, τ_i corresponds to t_i, and $-1 \leq \tau_i \leq 1$.

Now, (4) is used to compute the *A*-transform **x** of $x(t)$ on the subinterval k-$n_A \leq t \leq k$+1 of k-$m \leq t \leq k$+1 in terms of the vector $\mathbf{x}_{aux}$ defined in (1). The result is the following relation

$$\mathbf{x} = \mathbf{C}(m, n_A)\,\mathbf{x}_{aux}, \tag{12}$$

which defines the *A-interpolation matrix operator* $C(m,n_A)$.

As the *A*-transform reduces the computation of the response of the analog filter $H(s)$ to a linear algebra problem, a first general expression for the A-transform $\mathbf{y} = Ay(t)$ is obtained,

$$\mathbf{y} = -\mathbf{G}\,\mathbf{y}_{aux} + \mathbf{F}\,\mathbf{x}_{aux}. \tag{13}$$

The parameters G and F in (13) are calculated once and for all for any given transfer function $H(s)$. Then, the inverse A-transform (10) is to be applied to both sides of (13) in order to yield $y(t)$ at any desired time instant k-$n_A \leq t \leq k$+1. In particular, the choice $t=k$ provides the conventional digital filter difference equation

$$y_{k-d} = -\mathbf{g}^{\mathrm{T}}\,\mathbf{y}_{aux} + \mathbf{f}^{\mathrm{T}}\,\mathbf{x}_{aux}. \tag{14}$$

Likewise, any fixed fractional prediction time like f_P in Fig. 1 yields a pair $\{\mathbf{g},\mathbf{f}\}$ of vectors which can be pre-computed and saved. A different problem arises when f_P is variable and must be determined in real time, during each sampling interval. An efficient solution, which avoids the recalculation of **g** and **f** from G and F, is available based on the *time-window contraction matrix* S (see, e.g., [7]) which relates the *A*-transforms **y** and $\mathbf{y}_C$, respectively defined on the intervals $-1 \leq \tau \leq 1$ and $-1 \leq \tau_f \leq 1$ in Fig. 1: $\mathbf{y}_C = \mathrm{S}\,\mathbf{y}$. Now, the solution (13), together with the matrices $C_y = S\,G$ and $C_x = S\,F$, is calculated once and for all, under the assumption that the *output interval* is placed as in Fig. 1 and only f_P is variable.

IV. MAIN PROPERTIES OF THE G-EWD METHOD

The theoretical considerations presented below, as well as extensive numerical tests, support the conclusion that the G-EWD transfer functions are near-optimal equivalents of their analog counterparts. While the corresponding digitizing errors are always comparable to those of the digital equivalents designed iteratively with the traditional WLS frequency sampling method [3], the G-EWD method has two salient features with practical implications. First, since both the analog and digital transfer functions are analytical rational functions, the properties of such functions dramatically simplify the design problem relatively to the WLS design which is meant to approximate arbitrary frequency responses. Specifically, there is no more need for the iterative refinement typical of the WLS design. Second, in contrast to the design performed directly in the digital domain, the nature of these digitizing equations which approximate the output signals of analog filters leads to an efficient solution to the problem of implementing a fractional-time prediction by digital means.

A. Properties Related to the Interpolation Space

Consistently with the approach taken in this paper, the digital system design problem is restricted to the problem of approximating the transfer function (2) of an analog system of order n_A by a discrete-time transfer function

$$H_D(z) = \frac{p_0 z^m + p_1 z^{m-1} + \ldots + p_m}{z^{m-n_A}(z^{n_A} + g_1 z^{n_A-1} + \ldots + g_{n_A})} = \frac{N_D(z)}{D_D(z)}, \qquad (15)$$

where $m \geq n_A$. This is a problem of complex approximation in the unit disk by rational functions that is solved through interpolation such that the interpolation points are also in the unit disk in the G-EWD case, but are on the unit circle in the case of the T-EWD. Since both $H(s)$ and $H_D(z)$ are analytical rational functions, the properties of analytic functions imply some rather powerful constraints on their behavior within their respective regions of convergence. Moreover, these constraints also restrict the behavior of $H(j\omega)$ and $H_D(e^{j\omega})$ leading, for example, to the relationships between their real and imaginary parts, as well as their magnitudes and phase angles. One more consequence of the constraints on the transfer functions $H(s)$ and $H_D(z)$ relates their poles through the relationship $z_n = e^{\lambda_n}$, mentioned in Property P1 above. This is equivalent to the time domain condition that the modes z_n^k of the digital system are exactly the same as the sampled sequences of the modes $e^{\lambda_n t}$ of the analog prototype. Thus, although the analyticity properties imply that $H(s)$ and $H_D(z)$ can be completely defined by their behavior within any restricted domain of analyticity in the unit disc, the EWD design is simplified by the pole-matching condition to the extent that there is no need for an iterative refinement as in the general WLS design.

In practice, the above considerations are to be viewed in the context of the inherent aliasing of the digitizing techniques, and so the selection of the interpolation space basis will depend on the specifications of $H(s)$. Thus, in the case of high quality single-band filters primarily encountered in digital communication systems, the T-EWD is the method of choice. The latter is a particular case of the G-EWD method applied to an interpolation space spanned by a set of sinusoids whose frequencies are chosen within the frequency range $[\omega_0, \omega_M]$ that contains most of the spectral energy of $H(j\omega)$. Relevant examples were given in [1] and [2]. On the other hand, the special G-EWD design that uses the interpolation space spanned by the modes of the $H(s)$ yields significantly better results than the T-EWD in the case of the transfer functions that are encountered in the control system design. This is illustrated in Figs. 3 and 4 for the transfer function

$$H(s) = \frac{4000\,(s+6)\,(s+7)\,(s^2+s+8)}{(2s^2+s+4)\,(2s^2+s+8)\,(s^2+s+380)\,(s^2+s+400)}. \qquad (16)$$

Indeed, Fig. 3 evidences the fact that six frequency knots chosen within the excessively narrow frequency range $[0,0.25]\,\%\,\omega_f$ still provide a reasonably good transfer function $H_D(z)$ consistently with the analysis based on the analyticity properties. Nevertheless, the digitizing error around the second peak of the magnitude plot was greater than the errors of the designs represented in Fig. 4, and so it was not shown in this figure. Instead, the better error of a T-EWD filter derived with the wider frequency range $[\omega_0, \omega_M] = [0,0.7]\,\omega_f$ was shown with the dashed line. Thus, Fig. 4 illustrates the fact that the G-EWD method based on the modes of $H(s)$ provides better results in the case of systems characterized by wideband frequency responses as, for example, continuous-time state observers.

B. Noniterative Digitizing of Analog Systems

Similar considerations led to the conclusion [2] that the T-EWD and WLS designs were equivalent, and so the T-EWD method represented an accurate noniterative alternative. In fact, it was proven in [2] that the T-EWD digital equivalents are rigorously identical to those designed with a WLS method performed with the imposed poles $z_n = e^{\lambda_n}$.

The WLS minimizes the relation

$$\min_{p_\ell,\, g_\ell} \sum_{n=0}^{M} w(\omega_n) \left| H(j\omega_n) - H_D(e^{j\omega_n}) \right|^2, \qquad (17)$$

where p_ℓ and g_ℓ are the unknown coefficients of the numerator and denominator of $H_D(z)$, ω_n are the frequency knots within $[0,\pi]$, and $w(\omega)$ is a user defined weighting function. As the design considered in this paper deals with the problem of approximating the transfer function of an analog system by a discrete-time transfer function, the analyticity properties discussed above state that the denominator of $H_D(z)$ is uniquely computed through the mapping defined in Property P1.

Also, extensive tests done on the G-EWD and WLS designs supported this assertion, in the sense that all the denominators were practically the same. Only when a large number M is chosen in (17), the WLS design might lead to slightly different numerators, while the digitizing error $E_D(\omega) = 20 \log_{10}(|H(j\omega) - H_D(e^{j\omega})|)$ remains in about the same range as the G-EWD error.

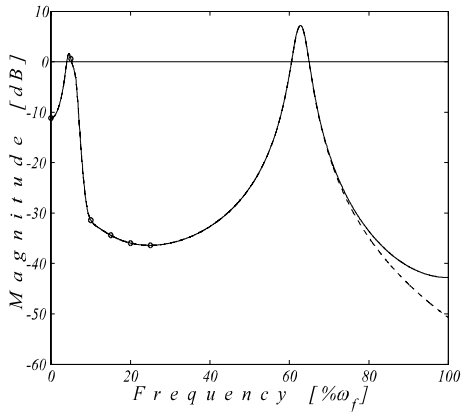

Fig. 3 Normalized responses $H(j\omega)$ (solid line), and $H_D(e^{j\omega})$ (dashed line) for the system defined by (16) with sampling period T_s=0.1 sec and ω_f=10π rad/sec. $H_D(e^{j\omega})$ was derived with the T-EWD method using the six frequency knots shown (small circles). Since the G-EWD plot overlaps here the $H(j\omega)$ plot, the G-EWD design is assessed in Fig. 4.

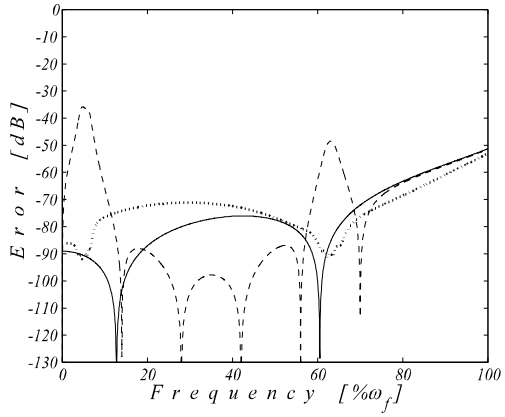

Fig. 4. The digitizing error $E_D(\omega)$ of three digital equivalents to the transfer function $H(s)$ shown in Fig.3 (n_A=8, m=11, d=0): the G-EWD equivalent designed with the eight modes of $H(s)$ and two sinusoids with frequencies 0.15 ω_f, and 0.64 ω_f (solid line); the T-EWD equivalent designed with the frequency range $[\omega_0, \omega_M]$=[0,0.7]ω_f (dashed line); the digital equivalent given by an iterative WLS method (dotted line).

The filter designed with an iterative WLS method is compared in Fig. 4 to the G-EWD filter designed with the eight modes of $H(s)$ and two sinusoids selected as to reduce the digitizing error. Thus, Fig. 4 supports the assertion that the G-EWD method provides results that are comparable to the optimal solution produced with the iterative WLS digitizing method. The latter is used here as a benchmark for the assessment of the proposed design since it is well known that it is definitely superior to the traditional bilinear transformation or the impulse- and step-invariance methods.

V. CONCLUSION

An interpolation based digitizing method was developed in this paper by using a general interpolation space spanned by a set of linearly independent functions of time. In the case of control system applications where the digital equivalent $H_D(z)$ of a transfer function $H(s)$ is required, the modes of $H(s)$ provide a natural basis for the interpolation space. The proposed G-EWD produces a digital equivalent defined through two sets of equations: (i) the conventional I/O recursive equation (14), also defined by the transfer function $H_D(z)$ in (8) and (9), and (ii) the fractional-time interpolation matrix equation (13). The matrices G and F in (13) can be stored with reduced-word arithmetic, since they correspond to a narrow A-transform interval. Moreover, if only one predicted value is to be computed as, for example, at the time instant $(k+f_P)$ in Fig. 1, then G and F are vectors of lengths n_A and m, respectively. While any digitizing method is characterized by some kind of output prediction on the time interval $k\text{-}1 \le t \le k$, what makes the prediction estimation of the G-EWD uniquely accurate is precisely the extended interpolation interval which allows for the particular set of initial conditions $y(k\text{-}n_A), \ldots, y(k\text{-}1)$ that form a natural match to the initial conditions of the analog system as opposed to a sequential approach that would cascade the interpolator and $H(s)$.

Apparently, the G-EWD approach makes the approximation $y(t)$ benefit of the increased accuracy of the central part of the m-segment interpolation interval which contains most of the signal energy. Finally, the fact that the T-EWD and WLS filters are equivalent [2] suggests that the G-EWD filters are near-optimal as well, and so they are not only efficient tools for applications that require fractional-time prediction but also very accurate digital equivalents of the original analog system and are obtained through a noniterative design.

REFERENCES

[1] G.I. Braileanu, "Extended-Window Interpolation Applied to Digital Filter Design," *IEEE Trans. Signal Processing*, vol. 44, pp. 457-472, March 1996.

[2] G. I. Braileanu, "Equivalence Between the Extended Window Design of IIR Filters and Least Squares Frequency Domain Designs," in *Proc. 2003 Int. Conf. on Acoustics, Speech, and Signal Processing* (*ICASSP* 2003), vol. VI, pp. 21-24, Hong Kong, 2003.

[3] C.S. Burrus, T.W. Parks, *Digital Filter Design*, Wiley, 1987.

[4] G. F. Franklin, J. D. Powell, and M. L. Workman, *Digital Control of Dynamic Systems*, Menlo Park, CA: Addison Wesley, 1998.

[5] R. E. Ziemer, W. H. Tranter, and D. R. Fannin, *Signals and Systems: Continuous and Discrete*, Upper Saddle River, NJ: Prentice Hall, 1998.

[6] M.J.D. Powell, *Approximation Theory and Methods*, Cambridge Univ. Press, 1981.

[7] G. Braileanu, "Matrix Operators for Numerically Stable Representation of Stiff, Linear Dynamic Systems," *IEEE Trans. on Automatic Control*, vol. AC-35, pp. 974-980, August 1990.